The Stabilization Effect of CO_2 Chemistries in Li-O_2/CO_2 Batteries

Kai Chen[a,b,+], Gang Huang[c,+], Jin-Ling Ma[a], Jin Wang[a], Dong-Yue Yang[a,b], Xiao-Yang Yang[a], Yue Yu[a,b], and Xin-Bo Zhang[a,b,*]

[a] K. Chen[+], J.-L. Ma, J. Wang, D.-Y. Yang, X.-Y. Yang, Y. Yu, Prof. X.-B Zhang
State Key Laboratory of Rare Earth Resource Utilization, Changchun Institute of Applied Chemistry, Chinese Academy of Sciences, Changchun, Jilin 130022, China.
E-mail: xbzhang@ciac.ac.cn
[b] K. Chen[+], D.-Y. Yang, Y. Yu, Prof. X.-B Zhang
University of Science and Technology of China, Hefei, Anhui 230026, China.
[c] G. Huang[+]
Physical Science and Engineering Division, King Abdullah University of Science and Technology, Thuwal, 23955-6900, Saudi Arabia.
[+] These authors contributed equally to this work.

Abstract: The lithium (Li)-air battery possesses ultrahigh theoretical specific energy, however, even in pure oxygen (O_2), the vulnerability of conventional organic electrolytes and carbon cathodes towards reaction intermediates, especially O_2^-, and corrosive oxidation and crack/pulverization of Li metal anode lead to poor cycling stability of the Li-air battery. Even worse, the water and/or CO_2 in air are reported to bring more serious parasitic reactions and security issues. Therefore, most significant improvements are achieved in pure O_2, and thus the making "onboard" pure oxygen supply system is inevitable for practical Li-air battery, which not only reduces the energy density of the overall system, but also makes the system complex and expensive to produce and maintain. Therefore, realizing the ultimate goal of applying such systems in open-air environment is a demanding requirement. Here, contrary to previous assertions, we found that CO_2 could improve the stability of both anode and electrolyte, and a high-performance rechargeable Li-O_2/CO_2 battery is then developed. The introduced CO_2 can not only facilitate the *in situ* formation of a passivated protective Li_2CO_3 film on Li anode, but also restrain side reactions involving electrolyte and cathode by capturing O_2^-. Moreover, the Pd/CNT catalyst in cathode can extend the battery lifespan by effectively tuning the product morphology and catalyzing the decomposition of Li_2CO_3. By simultaneously addressing the bottleneck problems of poor rechargeability, instability of carbon cathode, liquid electrolyte and Li anode, the designed Li-O_2/CO_2 battery achieves a full discharge capacity of 6,628 mAh g^{-1} and a long life of 715 cycles, which is even better than those of pure Li-O_2 batteries. When extending the concept to other important metal-air systems including Na-O_2/CO_2 and K-O_2/CO_2 batteries, the electrochemical performances are also greatly improved compared with those of Na/K-O_2 batteries, proving the general effectiveness of the strategy. We believe the findings here present an important step towards Li-air batteries from Li-O_2 batteries as well as other metal-air systems.

Introduction

Pursuing energy storage systems with higher energy densities has never stopped since last century, and this trend has been accelerated by the fast development of clean energy utilization and electronic devices and vehicles in recent years. Among the large number of available choices, the ultrahigh theoretical specific energy density (~3500 Wh/kg) of Li-air battery makes it an ideal candidate for next-generation energy supplier.[1] However, many challenges are waiting to be resolved before Li-air batteries can be applicable.

A Li-air battery usually composes of a porous carbon material as air electrode, a nonaqueous electrolyte and a Li plate as anode. During discharge, O_2 from air can react with Li^+ to form Li_2O_2, which subsequently decomposes during recharge. [1b, 1c] Despite the overall reaction is simple, even in pure oxygen (O_2), the vulnerability of conventional organic electrolytes and carbon cathodes towards reaction intermediates, especially O_2^-, and the corrosive oxidation and crack/pulverization of Li metal anode render the system complicated and severely limit the cycling stability of the Li-air battery.[2] Currently, no method can solve these problems simultaneously. The situation is even worse when operating the system in air, since the H_2O and/or CO_2 in air are reported to bring more serious parasitic reactions and security issues. [3] As a result, most significant improvements have been achieved in pure oxygen to avoid these issues,[4] applying these kinds of Li-O_2 batteries in practical condition will reduce the overall energy density and increase the cost because of the O_2 supply systems. Therefore, realizing the ultimate goal of applying such system in open-air environment is a demanding requirement.

Many groups noticed that CO_2 could deteriorate the battery performances, and they claimed that CO_2 participated in the discharge process in a complexed way to form Li_2CO_3, which was more difficult to be decomposed than Li_2O_2[3c, 5]. This results in high charge overpotentials, low coulombic efficiencies (CEs) and short battery lifespan. Therefore, researchers suggest that CO_2 should be completely removed from the Li-air batteries to make the reactions easier. [3a-c, 5a, 6] Based on these results, the impact of CO_2 seems to be fully understood and subsequently, the investigations on CO_2 in Li-O_2 batteries have not received much attention. However, CO_2 is an indispensable component in air, we cannot bypass this obstacle on the way towards Li-air battery, thus devoting efforts to unveiling the true role of CO_2 is critical.

Contrary to previous assertions, here we found that CO_2 could improve the stability of the battery components, including cathode, electrolyte and Li anode. It is well known that the side product, Li_2CO_3 in Li-O_2 batteries is stable with electrolytes and cathodes while the discharge product of Li_2O_2 is not. [7] Since the product in our Li-O_2/CO_2 battery is solely Li_2CO_3, the battery stability can be boosted. Furthermore, CO_2 can promote the formation of Li_2CO_3 on the Li surface to protect it from H_2O and other offensive intermediates. The mechanism of Li_2CO_3 formation is then discussed in detail. After in-depth research in the stability of cathode and electrolyte by NMR and FTIR, it has also been confirmed that CO_2 can capture O_2^- to reduce its nucleophilicity. Therefore, the introduction of CO_2 into the O_2 reaction gas stabilizes the whole battery system, and thus a high performance Li-O_2/CO_2 battery has been obtained. In addition, we have added CO_2 in Na (K)-O_2 batteries and the performances have been greatly improved as well.

Results and Discussion

A prototype ECC-AIR Li-O_2/CO_2 battery was assembled based on Pd/CNT cathode with flowing O_2/CO_2 (1:1) at 1 atm. The composition and structure information of the synthesized Pd/CNT can be found in Figures S1-S3 and the structure of ECC-AIR type cell is shown in Figure S4. Compared with CNT cathode, an obvious decrease in charge overpotential can be observed for the Pd/CNT cathode (Figure S5), revealing its effectiveness in promoting the decomposition of the discharge product. The evolution of Pd/CNT cathode after discharge and charge has been recorded by FTIR and Raman spectra. In the FTIR spectra (Figure 1A), typical peaks at 1437 cm^{-1} and 878 cm^{-1} corresponding to Li_2CO_3 appear in the discharged cathode and these peaks almost vanish after subsequent recharge, implying the formed Li_2CO_3 discharge product can be reversibly decomposed during the charge process. Similar results can also be observed in the Raman spectra with the emergence and disappearance of the Li_2CO_3 peak at 1084 cm^{-1} in the discharged and recharged cathodes (Figure 1B). SEM characterization was then conducted to further confirm the formation and decomposition of Li_2CO_3 during the cycling process of the Li-O_2/CO_2 batteries (Figures 1C-1E). A more detailed evolution of the discharge product can be seen in Figure S6. All these results affirm that the designed Li-O_2/CO_2 battery permits reversible formation and decomposition of Li_2CO_3.

It is widely accepted that the discharge reaction proceeds according to Eq. 1 in Li-O_2 batteries.

$$2Li + O_2 \rightarrow Li_2O_2 \quad (1)$$

While in the Li-O_2/CO_2 battery, since the gas atmosphere has been changed to O_2/CO_2 (1:1), the fundamental reaction mechanisms are still unclear. To elucidate this, operando pressure test has been conducted (Figure S7). As a comparison, the pressure change during cycling of Li-O_2 battery has also been given. From Figure 1F we can see that the Li-O_2 battery follows the 2.07 e/O_2 coefficient during discharge, in line with the theoretical value of 2 e/O_2 in Eq. 1. With the introduction of CO_2 into the reaction gas, the number of electrons transferred per gas molecule changes to 1.30 (1.30 e/gas) during discharge of the Li-O_2/CO_2 (1:1) battery (Figure 1G). Considering that Li_2CO_3 is the exclusive discharge product as above proved, the overall discharge reaction formula in Li-O_2/CO_2 (1:1) battery is as follows (Eq. 2), whose theoretical value is 1.33 e/gas.

$$2Li + 1/2O_2 + CO_2 \rightarrow Li_2CO_3 \quad (2)$$

It is obvious that the pressure cannot recover to the initial states in both Li-O_2 and Li-O_2/CO_2 batteries after recharging the same capacity, probably due to the existence of side reactions. The side reactions are resulted from the electrolyte decomposition and/or carbon degradation induced by the intermediates, O_2^-, $^1O_2$, etc. [8] In the first charge, 6.02 e/gas and 3.17 e/gas are achieved respectively in the Li-O_2 and Li-O_2/CO_2 batteries, indicating more parasitic reactions happen in the Li-O_2 battery than in the Li-O_2/CO_2 battery. The differential electrochemical mass spectra (DEMS) during charge of Li-O_2/CO_2 battery was then tested. The generation of O_2, CO and CO_2 as well as some fragments resulted from electrolyte decomposition can be clearly observed from Figure S8, confirming the occurrence of side reactions.

In Li-O_2 batteries, the Li anodes are easy to be corroded by H_2O, generating porous LiOH layer, [2a] which allows H_2O to continuously diffuse across, and thus constantly consuming the remaining Li anode and finally leading to the exhaustion of the Li anode and death of the batteries. When disassembling the cycled Li-O_2/CO_2 battery, we found that the Li anode was very stable in this system without corrosion. Figure 2A vividly shows the difference of the Li anodes after cycling in Li-O_2 and Li-O_2/CO_2 batteries. To clarify the origin of this phenomenon, the cycled Li anode in Li-O_2/CO_2 battery has been systematically characterized. Figures 2B and 2C give the C 1*s* and Li 1*s* XPS spectra of the cycled Li anode. The strong C 1*s* and Li 1*s* peaks of Li_2CO_3 at 289.6 and 55.1 eV can be clearly observed,[1f] confirming the formation of Li_2CO_3 on the Li anode surface. The other C 1s peaks show the CH_3OCO_2Li at 287.9 eV and C-C bond at 284.8 eV, which may arise from the SEI film formed on the Li surface.[9] Moreover, the Raman spectrum of the cycled Li anode also reveals a Li_2CO_3 peak at 1,084 cm^{-1} (Figure 2D), which is consistent with the XPS results.

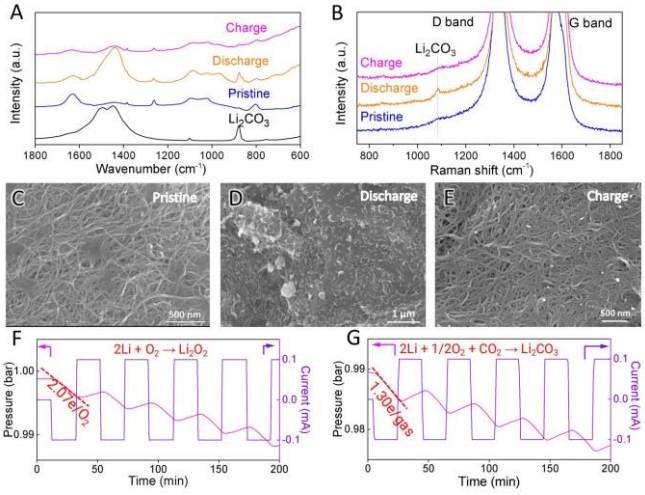

Figure 1. The rechargeability of Li-O_2/CO_2 battery. (A) FTIR spectra and (B) Raman spectra of the pristine, discharged and charged cathodes. (C-E) The corresponding SEM pictures of the cathodes. (F) The pressure change during cycling of Li-O_2 battery. (G) The pressure change during cycling Li-O_2/CO_2 battery. Current density is 0.1 mA (88.5 μA cm^{-2}) for F and G.

The SEM image in Figure 2E displays that nanosheet-like, dense Li_2CO_3 covers the surface of the cycled Li anode, which can be further confirmed by the zoom-out SEM images in Figures S9A and 9B. However, the cycled Li anode in Li-O_2 battery exhibits a porous surface composed of LiOH (Figures S9C and 9D). The surface morphology of the Li anode after cycling in Li-O_2/CO_2 battery is similar with the paper reported by Asadi Mohammad et al.[1f] Nevertheless, the Li anode protection induced by our design is much easier without the need of pre-cycling the Li anode in another system and tedious battery assembly and disassembly processes.

The Li anode protection effects induced by different systems are further compared in Figure 2F by exposing the original Li plate and the Li plates cycled in Li-O_2/CO_2 and Li-O_2 batteries to open air. It can be observed that, even after 60 min, the Li_2CO_3 protected Li plate still not totally darken and the central part remains stable, demonstrating the superior stability of the Li plate cycled in Li-O_2/CO_2 battery than that cycled in Li-O_2 battery. Moreover, the anode protection effect in our system can be reinforced with the increase of cycle number, because the protective Li_2CO_3 will continuously form on the Li anode surface (Figure 2G and Figure S10). By comparing the Li anodes after cycling in Li-O_2 and Li-O_2/CO_2 batteries for 120 h, Figure S11 demonstrates the vital role of the CO_2 for protecting the Li anode.

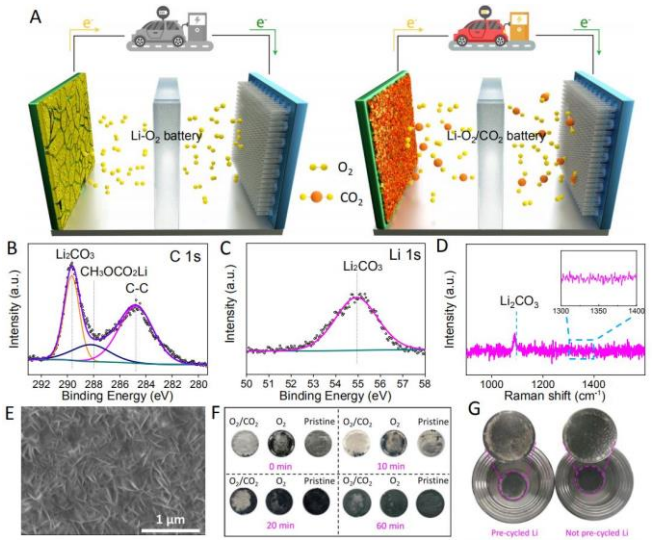

Figure 2. Characterizations of the Li anode after cycling in Li-O_2/CO_2 batteries. (A) Schematics of the Li anode in Li-O_2 battery and the Li_2CO_3 protection effect on the Li anode in Li-O_2/CO_2 battery. (B-E) XPS spectra of C 1*s* and Li 1*s*, Raman spectrum and SEM image of the Li anode after cycling in Li-O_2/CO_2 battery. (F) Li anode stability towards air after cycling in Li-O_2/CO_2 and Li-O_2 batteries for 80 h. The time on the picture means the exposure time in air (relative humidity: 40%). (G) The optical pictures of Li anodes after 100 h running in the Li-O_2 batteries with pre-cycled Li anode in Li-O_2/CO_2 battery and uncycled Li anode. The pre-cycled Li anode ran in Li-O_2/CO_2 battery for 80 h and the uncycled Li anode was rested at the same situation for 80 h.

Note that the Li_2CO_3 layer is very useful for protecting the Li anode, we need to elucidate its formation mechanism. There are three possible routes for the formation of Li_2CO_3 film (Table 1). The first route is the direct reaction between Li and CO_2 to form C and Li_2CO_3. According to the Raman result in Figure 2D, no peaks for C are detected, so route I can be ruled out. The difference between routes II and III is whether O_2 or H_2O participates in the reactions. This can be identified by whether cycling is requested for the formation of Li_2CO_3 layer, because H_2O mainly comes from electrolyte decomposition during cycling. A contrast experiment was conducted by using two Li-O_2/CO_2 batteries: one resting for 80 h while the other one cycling for 80 h. Subsequently, the gas environment of the batteries was changed to pure O_2. After cycling for another 100 h, the pre-cycled Li anode is less corroded compared with the resting Li anode (Figure 2G), which is completely dark without observable protection effect, and is very similar to the Li anode in Li-O_2 battery without resting in O_2/CO_2 (see Figure S11A). Even though pre-cycling of Li anode in Li-O_2/CO_2 battery can generate Li_2CO_3 protection layer, the Li anode can still be corroded during cycling in Li-O_2 battery by the penetration of H_2O across the Li_2CO_3 film in the long run, indicating that the presence of CO_2 is indispensable for the continuous anode protection. Another comparison by resting the Li anodes in Li-O_2/CO_2 and Li-O_2 batteries further confirms that the Li_2CO_3 protection film cannot be formed by simply stewing Li anode in Li-O_2/CO_2 battery (Figure S12). These experiments indicate that cycling is indispensable for the formation of Li_2CO_3 protection film, in other words, the H_2O generated by the decomposition of the electrolyte during cycling is critical for the formation of Li_2CO_3 protection film. Therefore, route II can be excluded. The H_2O in the cycled battery will react with Li anode to form LiOH and H_2, followed by the reaction between LiOH and CO_2. Since the reactions in route III is very fast, CO_2 can capture LiOH once it forms.[10] On the basis of above analysis, we speculate that route III is the most reasonable mechanism for the Li_2CO_3 formation on the Li anode. Furthermore, to directly visualize the CO_2 induced protective effect on Li anode, a simulation experiment has been designed, please see the results and discussions in Figure S13. In addition, we also immersed Li plates in the electrolytes pre-saturated with O_2 and O_2/CO_2 and exposed them to air. As indicated in Figure S14, the Li plate can be stabilized more than 10 days with the help of CO_2.

Table 1. Proposed routes for the formation of Li_2CO_3 on Li anode.

Routes	Reactions
I	$4Li + 3CO_2 \rightarrow 2Li_2CO_3 + C$
II	$2Li + ½O_2 + CO_2 \rightarrow Li_2CO_3$
III	$Li_{(s)} + H_2O_{(sol)} \rightarrow LiOH_{(sol)} + ½\ H_{2(g)}$ $2LiOH_{(sol)} + CO_{2(sol)} \rightarrow Li_2CO_{3(s)} + H_2O_{(s)}$ Total: $2Li_{(s)} + H_2O_{(sol)} + CO_{2(sol)} \rightarrow Li_2CO_{3\ (s)} + H_{2(g)}$

Superoxide radical, a strong nucleophilic reagent, has been widely proved to be the main origin of side reactions in Li-O_2 batteries, including electrolyte decomposition and cathode oxidation.[2b, 2c, 11] Therefore, capturing superoxide is very meaningful to stabilize the battery system. Back to 1984, Julian L. R. confirmed that O_2^- was prone to bind CO_2 through reactions in Eqs. 3 and 4 [12], which was further supported by the theoretical calculation conducted by Lim H. K.[5b] So we can reasonably speculate that CO_2 can capture O_2^- to reduce the disproportionation reaction in Li-O_2/CO_2 battery, thus parasitic reactions can be greatly alleviated (Figure 3A). Furthermore, since singlet oxygen, another cause for parasitic reactions in Li-O_2 batteries, forms by disproportionation of superoxide (O_2^-) (Eq. 5),[8c, 13] if O_2^- is captured, its disproportionation no longer happens, further reducing the side reactions.

$$O_2^- + CO_2 \rightarrow CO_4^- \quad (3)$$

$$CO_4^- + O_2^- + CO_2 \rightarrow C_2O_6^{2-} + O_2 \quad (4)$$

$$O_2^- + O_2^- \rightarrow O_2^{2-} + x^3O_2 + (1 - x)^1O_2 \quad (5)$$

The above speculation can be confirmed by comparing the ring current of the rotating ring-disk electrode (RRDE) in O_2 and O_2/CO_2 atmospheres. In the RRDE experiment, O_2 is first reduced to O_2^- at the disk, followed by the detection and oxidization at the ring. If the O_2^- is captured by CO_2, it cannot be oxidized anymore, thus there is almost no ring current can be detected. Figures 3B and 3C compare the ring currents in the O_2 and O_2/CO_2 systems. it is clear that the I_{ring} decreases sharply to nearly zero after involving CO_2, showing that CO_2 can indeed capture O_2^- (Figures 3B and 3C and Figure S15), in good consistence with previous reports. [12, 14] The stability of different electrolytes towards O_2^- and CO_2 captured O_2^- are compared and discussed in detail in Figure S16. The evolution of TEGDME electrolytes after cycling was checked by ^1H and ^{13}C nuclear magnetic resonance (NMR) spectra (Figures 3D and 3E). After discharge for 10 h, the electrolytes in both systems are decomposed with the appearance of new chemical shifts at 36 ppm in ^{13}C spectra and 2.6 ppm in ^1H spectra. As expected, the impurity peak intensities of Li-O_2/CO_2 battery are much lower than those of Li-O_2 battery. Furthermore, after 20 cycles, the differences are more obvious with almost no impurities can be seen for Li-O_2/CO_2 battery while peaks for the side products appear significantly in Li-O_2 battery. Even using commercial electrolyte, the Li-O_2/CO_2 battery still outlives the Li-O_2 battery (180 *vs.* 109 cycles, Figure S17) because of less electrolyte decomposition with the help of CO_2

induced stabilization effect. The above evidences demonstrate that the introduction of CO_2 into the reaction gas can effectively alleviate the electrolyte decomposition.

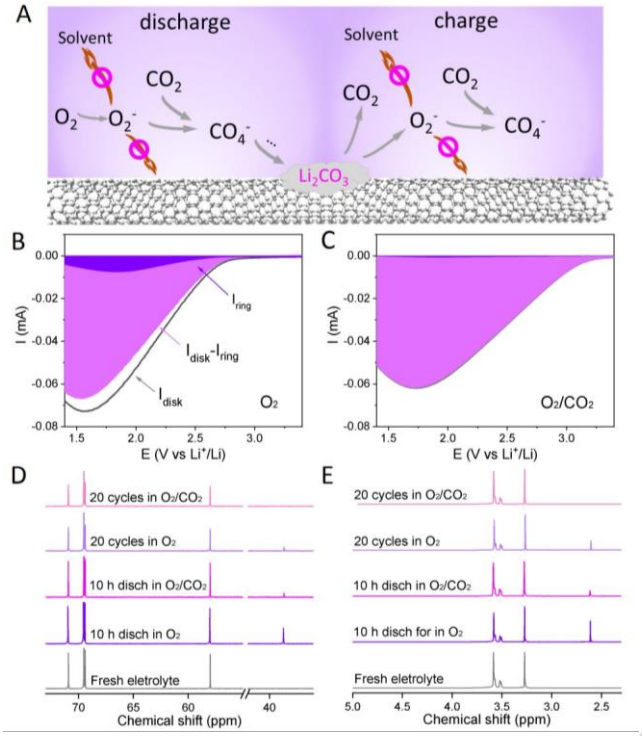

Figure 3. Schematic and confirmation of CO_2 endowed cathode and electrolyte stabilization in Li-O_2/CO_2 batteries. (A) The proposed reaction route of capturing O_2^- by CO_2. (B, C) The RRDE experiments in O_2 and O_2/CO_2 with 0.1 M $LiCF_3SO_3$/TEGDME electrolyte. (D, E) ^{13}C and ^1H NMR spectra of the cycled electrolytes dissolved in D_2O.

To confirm whether the side reactions can be attenuated at the cathode, the composition and morphology evolutions of the CNT and Pd/CNT cathodes at the end of discharge and charge states after multiple cycles were checked by FTIR and SEM. As indicated in the FTIR spectra in Figures 4A and 4B, after 10th discharge and charge, no obvious peaks corresponding to Li_2CO_3 and other species can be detected for CNT and Pd/CNT cathodes, probably due to the limited cycling capacity and good charge efficiency in this short cycle number. However, after 50 cycles, Li_2CO_3 peak at 880 cm^{-1} is clearly seen for CNT cathode, indicating the remnant of undecomposed Li_2CO_3 discharge product. In addition, C-O stretching vibrations related peaks around 940-1230 cm^{-1} and HCOOLi peak at 785 cm^{-1} also emerge, revealing the instability of CNT cathode and the electrolyte decomposition induced by high charge voltage or attacks from intermediate species during cycling.[15] In contrast to CNT cathode, there are no peaks at 940-1230 cm^{-1} or 785 cm^{-1} associated with the decomposition of CNT or electrolyte can be observed for Pd/CNT cathode after 50 cycles, manifesting its high stability to withstand the rigorous cycling conditions. Although Li_2CO_3 peak at 880 cm^{-1} appears at the 50th discharge, its intensity decreases after charge, disclosing the good catalytic effect of Pd/CNT. Similar results are also confirmed by Raman spectra in Figure S18. The discrepancy between CNT and Pd/CNT cathodes can be further clarified by SEM. After 10th discharge, the surfaces of the CNT and Pd/CNT cathodes are covered by amorphous Li_2CO_3 (Figures 4C and 4G). Then, most of the Li_2CO_3 product decomposes after 10th charge, leaving uncovered CNT and Pd/CNT cathodes (Figures 4D and 4H). Even after 50 cycles, the morphology of the Pd/CNT cathode can almost recover to the initial state (Figures 4I and 4J), revealing that Pd/CNT can effectively facilitate the decomposition of the Li_2CO_3 to extend the battery life, while the CNT cathode cannot recover after 50th charge (Figures 4E and 4F). The above results show minimal side products (HCOOLi and CH_3COOLi) originating from cathode and electrolyte decomposition in the Li-O_2/CO_2 battery with Pd/CNT cathode, which is superior to Li-O_2 batteries with severe side products just after 20 cycles,[15] proving the participation of CO_2 can truly stabilize the Pd/CNT cathode and reduce parasitic reactions.

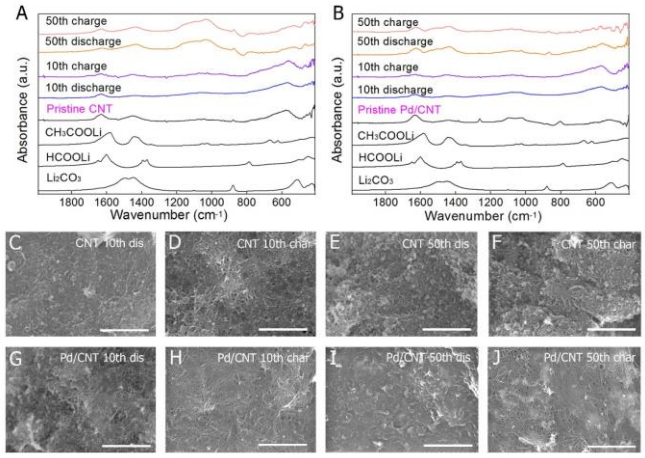

Figure 4. FTIR spectra and SEM pictures of cycled CNT and Pd/CNT cathodes at the end of discharge and charge states. (A, B) FTIR spectra of CNT and Pd/CNT cathodes. (C-F) SEM pictures of CNT. (G-I) SEM pictures of Pd/CNT. The batteries were cycled with a cutoff capacity of 1000 mAh g^{-1} at 500 mA g^{-1}. Scale bar: 2 μm.

Considering the high catalytic effect and stability of Pd/CNT cathodes, stabilized electrolytes and Li anodes in the Li-O_2/CO_2 batteries, their electrochemical performances need to be amply studied. Figure S19 has proven that O_2 is indispensable in the feeding gas to ensure a high capacity and CO_2 plays a positive role to further increase the capacity. Figure 5A compares the full discharge and charge performances of the CNT and Pd/CNT based Li-O_2/CO_2 batteries in a fixed voltage window of 2.0-4.5 V. In the 1st cycle, the Pd/CNT based battery achieves a high discharge capacity of 6628 mAh g^{-1}, much higher than the 4,384 mAh g^{-1} capacity of CNT based battery delivered. At 5th cycle, the capacity of Pd/CNT based battery fades to 2726 mAh g^{-1}, but still nearly two times the capacity of CNT based battery (1562 mAh g^{-1}). Moreover, at a limited cycling capacity of 1000 mAh g^{-1}, the battery with Pd/CNT cathode exhibits a lower voltage gap than the battery with CNT cathode: 1.68 V vs. 1.88 V (Figure S5). The 0.2 V difference, in the long run, can keep the decomposition of Li_2CO_3 at a lower charge potential to reduce electrolyte decomposition (Figure S20). After this, electrochemical impedance spectroscopy (EIS) analysis has been conducted to check the interfacial stabilities of the batteries at different stages (Figure 5B). Except for the initial stage, the interfacial impedance of the battery with Pd/CNT cathode is always lower than that of battery with CNT cathode, indicating more stable electrode/electrolyte interphases are formed in the Pd/CNT based battery.

Figures 5C and 5D give the cycling performance of Pd/CNT based Li-O_2/CO_2 batteries with fixed capacities of 500 and 1000 mAh g^{-1}, respectively. Accordingly, long cycling life of 715 and 255 cycles can be achieved for the batteries. As a comparison, the cycling performance of CNT based Li-O_2/CO_2 battery with a fixed capacity

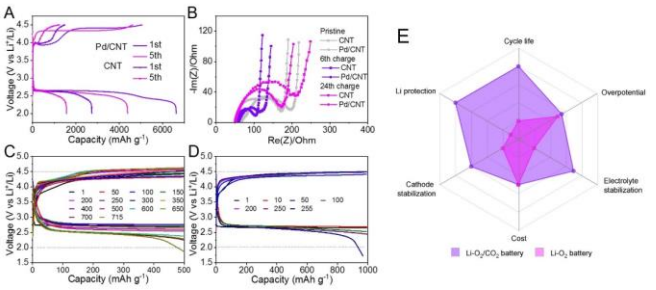

Figure 5. Electrochemical performances of Li-O_2/CO_2 batteries with CNT and Pd/CNT cathodes. (A) Full discharge and charge curves of the two batteries in a fixed voltage window of 2.0-4.5 V. (B) Electrochemical impedance spectroscopy (EIS) at initial stage, after 6th and 24th charge. (C) Cycling performance of Li-O_2/CO_2 battery with Pd/CNT cathode at a fixed capacity of 500 mAh g^{-1}. (D) Cycling performance of Li-O_2/CO_2 battery with Pd/CNT cathode at a fixed capacity of 1000 mAh g^{-1}. The current density is 500 mA g^{-1} for A-D. (E) A comparison of properties between Li-O_2 and Li-O_2/CO_2 batteries.

of 1000 mAh g^{-1} is shown in Figure S21A, which can only realize 56 cycles. For Li-O_2 battery with Pd/CNT cathode, it only runs for 94 cycles (Figure S21B), much shorter than the 255 cycles of Li-O_2/CO_2 battery. In addition, the terminal potential of charges experiences no obvious increase even changing the discharge product from Li_2O_2 in Li-O_2 battery to Li_2CO_3 in Li-O_2/CO_2 battery (Figure S21C). Excellent rate capability can also be realized in the Pd/CNT based Li-O_2/CO_2 batteries (Figure S22). These inspiring cycling and rate performances have never been achieved by previous Li-CO_2 (O_2) or Li-O_2/CO_2 batteries (see Table S1). Thanks to the synergistic effects of the Pd/CNT cathode and CO_2 enabled benefits on the whole battery, the cycling life of the designed Li-O_2/CO_2 battery even exceeds those of advanced Li-O_2 battery systems. [16] Although the charge overpotential of the Pd/CNT based Li-O_2/CO_2 battery is higher than some reported Li-O_2 batteries, its ultra-long lifetime can offset this disadvantage, because the price of consuming extra energy for charging the battery is much cheaper than the cost of manufacturing six new Li-O_2 batteries if we suppose a Li-O_2 battery can run for 100 cycles at the same condition. If intermittent energy (wind or solar energy) is employed, the cost can be further reduced. The cycling performances of Li-O_2 and Li-O_2/CO_2 batteries at higher capacities have also been compared in Figure S23. The performances of Li-O_2/CO_2 batteries again markedly exceed those of Li-O_2 batteries.

The above investigations are based on $LiCF_3SO_3$/TEGDME electrolyte, an electrolyte with low-donor-number (DN) TEGDME as solvent. To prove the universality of CO_2 induced electrochemical performance improvement, Li-O_2/CO_2 batteries with high-DN DMSO based electrolyte have been investigated (see details in Figures S24-S27). As expected, the introduction of CO_2 into the reaction gas not only promotes the lifetime but also elevates the energy efficiency of DMSO-based Li-O_2 batteries. The reason for the Li-O_2/CO_2 battery failure after 715 cycles has been investigated in detail (Figures S28-S30) and it is found that the failed cathode is the origin of the battery failure rather than the Li metal anode. Now that the Li-O_2/CO_2 battery can sustain such a long life, the Li anode stability after hundreds of cycles has been checked. Figure S31 demonstrates that the Li loss is only 6.23% after 500 cycles in the Li-O_2/CO_2 battery, making the Li plate can live more than 8000 cycles if the cathode is changed every 500 cycles. In sharp contrast, the Li plate in the Li-O_2 battery shows a high loss of 25.77% after just 50 times cycling and only 194 cycles can be achieved theoretically. The huge difference in Li loss between these two batteries can be explained by the anode stability revealed by Figure S32.

Above results have shown great success of introducing CO_2 into the Li-O_2 battery system. In view that high activity and instability of metal anodes is a common issue in metal-O_2 batteries, we hypothesize that this concept is applicable in other metal-O_2 battery systems, like Na-O_2 and K-O_2 batteries. Figures S33-35 give the cycling performance of Na/K-O_2 batteries with/without introduction of CO_2. The Na-O_2/CO_2 battery can sustain 129 stable cycles, two times that of Na-O_2 battery (62 cycles). More importantly, the K-O_2/CO_2 battery achieves a life of 294 cycles, far exceeding the 5 cycles of K-O_2 battery. The successful adoption of O_2/CO_2 in these two battery systems has proven the versatility of CO_2 usage in metal-air batteries.

Conclusion

In summary, we have demonstrated a high-capacity and long-life rechargeable Li-O_2/CO_2 (1:1) battery by using Pd/CNT as cathode. Thanks to the high catalytic Pd/CNT cathode, the Li_2CO_3 discharge product can be efficiently decomposed. The introduction of CO_2 into the feeding gas can induce a passivated Li_2CO_3 film formed on the Li anode surface during cycling, which can protect the Li anode from attacking by H_2O and intermediates. Moreover, the existence of CO_2 can also capture O_2^- to reduce side reactions related to electrolyte and cathode. Even though Li-O_2/CO_2 batteries have been reported previously, no researchers noticed the gas mixtures' protection effect on Li anode and stabilization role on electrolyte and cathode. We first propose and prove these new functions that CO_2 endows. Due to the synergistic optimizations brought by catalytic Pd/CNT cathode and CO_2, the Li-O_2/CO_2 battery achieves high performances with a full discharge capacity of 6628 mAh g^{-1} and a long life of 715 cycles. Instead of deteriorating the Li-O_2 batteries as people considered before, here CO_2 plays a positive role that promotes the battery performance and lifetime. Such a good performance has surpassed most of the state-of-the-art Li-O_2 batteries. Besides, the strategy we adopt here is applicable in other battery systems, like Na- and K-O_2/CO_2 batteries. We believe that this work deepens our understanding towards Li-O_2/CO_2 and Li-O_2 batteries, and makes an important attempt to prompt the applications of Li-O_2 batteries in open-air environments.

Acknowledgements

The authors thank the National Key R&D Program of China (2017YFA0206700), the National Natural Science Foundation of China (21725103), the Strategic Priority Research Program of the Chinese Academy of Sciences (XDA21010210) and the K. C. Wong Education Foundation (GJTD-2018-09)

Keywords: stabilization • Li-oxygen battery • carbon dioxide • side reaction prevention • superoxide capture

[1] a) P. G. Bruce, S. A. Freunberger, L. J. Hardwick, J. M. Tarascon, *Nat. Mater.* **2011**, *11*, 19-29; b) A. C. Luntz, B. D. McCloskey, *Chem. Rev.* **2014**, *114*, 11721-11750; c) J. Lu, L. Li, J. B. Park, Y. K. Sun, F. Wu, K. Amine, *Chem. Rev.* **2014**, *114*, 5611-5640; d) Z. L. Wang, D. Xu, J. J.

Xu, X. B. Zhang, *Chem. Soc. Rev.* **2014**, *43*, 7746-7786; e) Z. Lyu, Y. Zhou, W. Dai, X. Cui, M. Lai, L. Wang, F. Huo, W. Huang, Z. Hu, W. Chen, *Chem. Soc. Rev.* **2017**, *46*, 6046-6072; f) M. Asadi, B. Sayahpour, P. Abbasi, A. T. Ngo, K. Karis, J. R. Jokisaari, C. Liu, B. Narayanan, M. Gerard, P. Yasaei, X. Hu, A. Mukherjee, K. C. Lau, R. S. Assary, F. Khalili-Araghi, R. F. Klie, L. A. Curtiss, A. Salehi-Khojin, *Nature* **2018**, *555*, 502-506.

[2] a) J. L. Shui, J. S. Okasinski, P. Kenesei, H. A. Dobbs, D. Zhao, J. D. Almer, D. J. Liu, *Nat. Commun.* **2013**, *4*, 2255; b) S. A. Freunberger, Y. Chen, Z. Peng, J. M. Griffin, L. J. Hardwick, F. Barde, P. Novak, P. G. Bruce, *J. Am. Chem. Soc.* **2011**, *133*, 8040-8047; c) Y. Chen, S. A. Freunberger, Z. Peng, F. Barde, P. G. Bruce, *J. Am. Chem. Soc.* **2012**, *134*, 7952-7957.

[3] a) Y. C. Lu, E. J. Crumlin, T. J. Carney, L. Baggetto, G. M. Veith, N. J. Dudney, Z. X. Liu, Y. Shao-Horn, *J. Phys. Chem. C* **2013**, *117*, 25948-25954; b) Y. S. Mekonnen, K. B. Knudsen, J. S. G. Mýrdal, R. Younesi, J. Højberg, J. Hjelm, P. Norby, T. Vegge, *J. Chem. Phys.* **2014**, *140*, 121101; c) S. R. Gowda, A. Brunet, G. M. Wallraff, B. D. McCloskey, *J. Phys. Chem. Lett.* **2013**, *4*, 276-279; d) Z. Guo, X. Dong, S. Yuan, Y. Wang, Y. Xia, *J. Power Sources* **2014**, *264*, 1-7.

[4] a) J. Lu, Y. J. Lee, X. Luo, K. C. Lau, M. Asadi, H. H. Wang, S. Brombosz, J. Wen, D. Zhai, Z. Chen, D. J. Miller, Y. S. Jeong, J. B. Park, Z. Z. Fang, B. Kumar, A. Salehi-Khojin, Y. K. Sun, L. A. Curtiss, K. Amine, *Nature* **2016**, *529*, 377-382; b) T. Liu, M. Leskes, W. Yu, A. J. Moore, L. Zhou, P. M. Bayley, G. Kim, C. P. Grey, *Science* **2015**, *350*, 530-533; c) Z. Peng, S. A. Freunberger, Y. Chen, P. G. Bruce, *Science* **2012**, *337*, 563-566; dC. Xia, C. Y. Kwok, L. F. Nazar, *Science* **2018**, *361*, 777-781.

[5] a) W. Yin, A. Grimaud, F. Lepoivre, C. Yang, J. M. Tarascon, *J. Phys. Chem. Lett.* **2017**, *8*, 214-222; b) H. K. Lim, H. D. Lim, K. Y. Park, D. H. Seo, H. Gwon, J. Hong, W. A. Goddard, 3rd, H. Kim, K. Kang, *J. Am. Chem. Soc.* **2013**, *135*, 9733-9742; c) R. Wang, X. Q. Yu, J. M. Bai, H. Li, X. J. Huang, L. Q. Chen, X. Q. Yang, *J. Power Sources* **2012**, *218*, 113-118.

[6] G. Wang, L. Huang, S. Liu, J. Xie, S. Zhang, P. Zhu, G. Cao, X. Zhao, *ACS Appl. Mater. Interfaces* **2015**, *7*, 23876-23884.

[7] B. D. McCloskey, A. Speidel, R. Scheffler, D. C. Miller, V. Viswanathan, J. S. Hummelshoj, J. K. Norskov, A. C. Luntz, *J. Phys. Chem. Lett.* **2012**, *3*, 997-1001.

[8] a) N. Mahne, S. E. Renfrew, B. D. McCloskey, S. A. Freunberger, *Angew. Chem. Int. Ed.* **2018**, *57*, 5529-5533; b) S. X. Yang, P. He, H. S. Zhou, *Energy Environ. Sci.* **2016**, *9*, 1650-1654; c) N. Mahne, B. Schafzahl, C. Leypold, M. Leypold, S. Grumm, A. Leitgeb, G. A. Strohmeier, M. Wilkening, O. Fontaine, D. Kramer, C. Slugovc, S. M. Borisov, S. A. Freunberger, *Nat. Energy* **2017**, *2*, 17036; d) J. Wandt, P. Jakes, J. Granwehr, H. A. Gasteiger, R. A. Eichel, *Angew. Chem. Int. Ed.* **2016**, *55*, 6892-6895.

[9] L. Ye, M. Liao, H. Sun, Y. Yang, C. Tang, Y. Zhao, L. Wang, Y. Xu, L. Zhang, B. Wang, F. Xu, X. Sun, Y. Zhang, H. Dai, P. G. Bruce, H. Peng, *Angew. Chem. Int. Ed.* **2019**, *58*, 2437-2442.

[10] a) T. M. Ticich, *J. Chem. Educ.* **2011**, *88*, 189-191; b) Z. Zho, V. A. Chashchin, A. V. Vishnyakov, *Theor. Found. Chem. Eng.* **2007**, *41*, 577-584.

[11] a) R. Black, S. H. Oh, J. H. Lee, T. Yim, B. Adams, L. F. Nazar, *J. Am. Chem. Soc.* **2012**, *134*, 2902-2905; b) J. Lai, Y. Xing, N. Chen, L. Li, F. Wu, R. Chen, *Angew. Chem. Int. Ed.* **2019**, *58*, 2-26.

[12] L. R. Julian, Jr., S. C. Thomas, T. S. Donald, *J. Am. Chem. Soc.* **1984**, *106*, 4667.

[13] E. Mourad, Y. Petit, R. Spezia, A. Samojlov, F. Summa, C. Prehal, C. Leypold, N. Mahne, C. Slugovc, O. Fontaine, S. Brutti, S. A. Freunberger, *Energy Environ. Sci.* **2019**, *12*, 2559-2568.

[14] L. Johnson, C. Li, Z. Liu, Y. Chen, S. A. Freunberger, P. C. Ashok, B. B. Praveen, K. Dholakia, J. M. Tarascon, P. G. Bruce, *Nat. Chem.* **2014**, *6*, 1091-1099.

[15] J. J. Xu, Z. W. Chang, Y. Wang, D. P. Liu, Y. Zhang, X. B. Zhang, *Adv. Mater* **2016**, *28*, 9620-9628.

[16] a) Z. D. Yang, X. Y. Yang, T. Liu, Z. W. Chang, Y. B. Yin, X. B. Zhang, J. M. Yan, Q. Jiang, *Small* **2018**, *14*, 1800590; b) J. J. Xu, D. Xu, Z. L. Wang, H. G. Wang, L. L. Zhang, X. B. Zhang, *Angew. Chem. Int. Ed.* **2013**, *52*, 3887-3890; c) J. J. Xu, Z. L. Wang, D. Xu, F. Z. Meng, X. B. Zhang, *Energy Environ. Sci.* **2014**, *7*, 2213; d) Z. Jian, P. Liu, F. Li, P. He, X. Guo, M. Chen, H. Zhou, *Angew. Chem. Int. Ed.* **2014**, *53*, 442-446; e) F. J. Li, Y. Chen, D. M. Tang, Z. L. Jian, C. Liu, D. Golberg, A. Yamada, H. S. Zhou, *Energy Environ. Sci.* **2014**, *7*, 1648-1652.

Entry for the Table of Contents

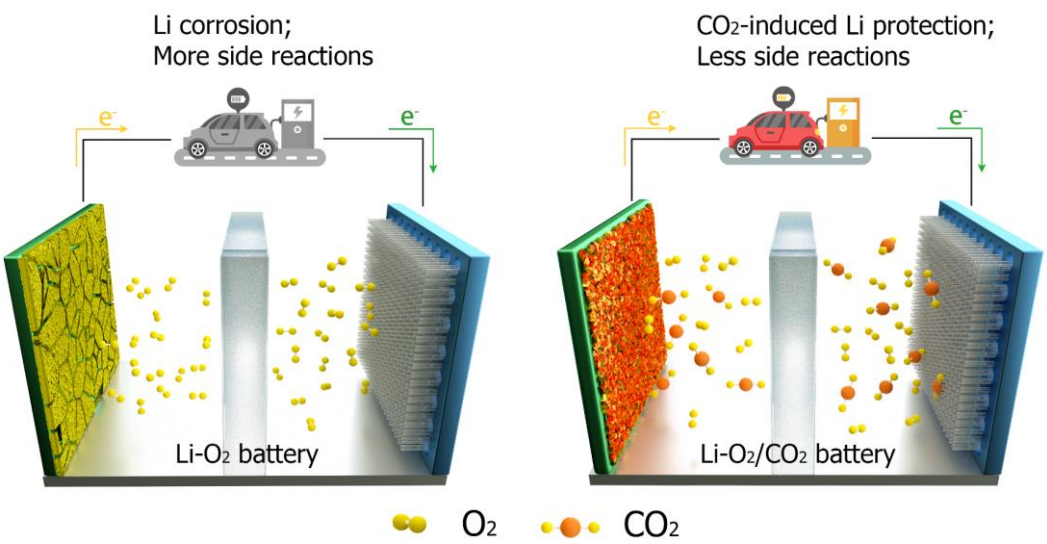

The application of Li-O_2 batteries is hindered by the anode corrosion and side reactions involving electrolyte and cathode. When they are operated in open air, the complex gas components (CO_2, H_2O, etc) will make the situation even worse. Carbon dioxide in air is previously considered detrimental to Li-O_2 batteries because of the Li_2CO_3 formation. However, here we found that CO_2 could make Li-O_2 battery more stable due to new chemistries CO_2 brings. On the anode side, CO_2 can facilitate the formation of a protective and self-healing Li_2CO_3 film, which can expel the H_2O and aggressive intermediates during cycling. As to cathode and electrolyte, they are also well protected since O_2^- intermediate is captured by CO_2 to reduce the nucleophilicity and prevent the formation of $^1O_2$. As a result, the CO_2 can suppress the side reactions and promote the stability of the Li-O_2 batteries to achieve excellent performance. After applying this concept in Na-O_2 and K-O_2 batteries, we confirm this idea can potentially make practical metal-air batteries more viable.